Transactions of the TSME (2017) Vol. 5, No. 1, 20-29
Journal of Research and Applications in Mechanical Engineering

ISSN 2229-2152 print
DOI:

Research Article

HEAT TRANSFER ENHANCEMENT IN LAMINAR FLOW OVER FLAT PLATE USING SMALL PULSATING JET

W. Rakpakdee
W. Chaiworapuek*
Department of Mechanical Engineering, Faculty of Engineering, Kasetsart University, 50 Ngamwongwan Road, Ladyao, Chatuchak, Bangkok, Thailand

ABSTRACT:
A technique of heat transfer enhancement over a heated plate using a water injection to disturb a laminar boundary layer is presented in this paper. The water jet was injected from the heated surface to the mainstream flow, having turbulence intensity of 1% through a 1 mm diameter hole. After the injection, a turbulent spot playing an important role on the heat transfer enhancement was generated artificially and investigated experimentally using thermochromic liquid crystals coated on the hot wall. In this study, contours of temperature and heat transfer coefficient were presented when the Reynolds number in the mainstream flow was varied as 117,000, 158,000, and 199,000 under the constant heat flux condition. The results show that this technique can increase heat transfer capability between the hot plate and freestream flow. The results from this research were found to be an important information that will be able to increase the efficiency of heat exchanger in the future.

Keywords: *Heat transfer, Turbulent spot, Flat plate, Reynolds number*

1. INTRODUCTION

The heat exchanger is widely used in many industrials such as air conditioning, refrigeration, and power plant etc. Thus, the cost of industrial processes can be directly decreased by increasing the efficiency of heat exchanger in their system. Normally, the techniques of heat transfer enhancement comprise the passive and active methods. The passive one is the technique that does not require external power source such as using fins, rough surface, swirler and nanoparticles. Meanwhile, the active technique employs the external power source, including electromagnetic field, jet, vibration and ultrasound. However, a pulsating jet, which is a technique requiring a very small input power to drive a jet was found to boost the rate of heat transfer on the flat plate. Therefore, this research investigates the thermal behavior on the flat plate after injecting a small pulsating water jet in the perpendicular direction of the mainstream at Reynolds number of 117,000, 158,000, and 199,000. With this injection, the laminar boundary layer is disturbed and a turbulent spot is created to gain the heat transfer rate. In this study, the thermochromic liquid crystals were fully coated on the entire test surface to measure the surface temperature. The image processing technique was utilized to extract the time- dependent thermal information. The obtained results are found to be an important data that will be able to increase the efficiency of heat exchanger in the future.

* Corresponding author: W. Chaiworapuek
E-mail address: fengwcc@ku.ac.th

2. TURBULENT SPOT

Typically, the fluid flow can be divided as three types, which are laminar, transition, and turbulent flows following the chaotic level. It can be classified using Reynolds number, Re. When the Re is less than the critical Reynolds number, the flow is considered as laminar flow. On the other hand, the flow is turbulent. With this assumption, the range of transition is ignored. The transition region on flat plate is divided into 4 regions following White [1]. The most important part was found to be able to increase the heat transfer capability via the turbulent spot, discovered by Emmons [2]. The structure of the turbulent spot is shown as Fig. 1.

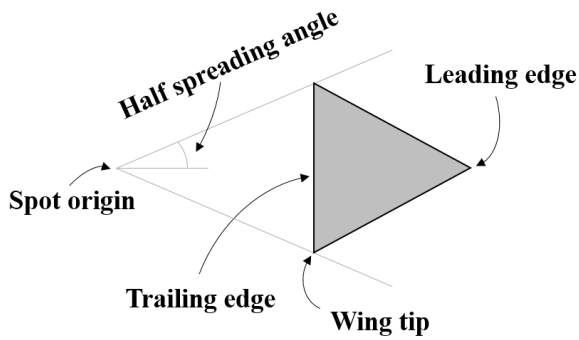

Fig. 1. Basic structure of turbulent spot.

The turbulent spot was found to have an arrowhead shape. Its leading edge has velocity of 0.74-0.89 of freestream velocity. Sabatino and Smith [3] found that the turbulent spot increases the heat transfer up to 15% above the laminar state at Re = 146,000. Also, Chaiworapuek and Kittichaikarn [4] showed that the turbulent spot at Re = 75,000 can boost the heat transfer rate up to 10%. Thus, the results obtained from this study will reveal the thermal behavior of the turbulent spot at different Re which has never been available before.

3. EXPERIMENTAL METHOD

3.1 Experimental setup

This experiment was conducted in closed-loop low freestream turbulence water tunnel. Fig. 2 shows a test section having width of 0.2 m x height of 0.15 m x length of 1 m. This section was made from 10 mm acrylic plate. The bleeding channel was set up at the inlet of test section to create a new boundary layer on the test plate. The flow rate was adjustable directly from an inverter to control 2.5 HP centrifugal water pump. With this method, the Re of the mainstream flow can be controlled as 117,000, 158,000, and 199,000 based on x = 1 m. The Re was determined from the water velocity, measured using a Nixon Streamflo velocity meter type 403 having an uncertainty of 0.35% at 0.5 m from the plate leading edge. The test plate was fabricated from 3 mm aluminum plate. At the bottom, a plate heater was installed to create a constant heat flux condition on the test plate. Also, a 1 cm aluminum plate was inserted between test plate and heater for a better distribution of the heat. Underneath the heater, a plate of thermal insulator was installed to resist the heat loss in downward direction. Then, a steel plate of 3 mm was assembled to strengthen the test plate. Above the flat plate, a black polyvinyl chloride sheet of 120 μm was well bonded to damp the heat, propagating in upward direction. In this research, the liquid crystals (TLCs) were used to show the temperature distribution on the test surface. They were fully coated over the test plate below the layer of vanish in order to prevent the degradation by the water. The TLCs in the present study is able to display the color as the function of the temperature between 26 – 30 ˚C. The type-K thin leaf thermocouples having an uncertainty of 0.75% were glued on top to measure the surface temperature at the streamwise position of 0.4 – 0.8 m from the plate leading edge with the interval of 0.1 m.

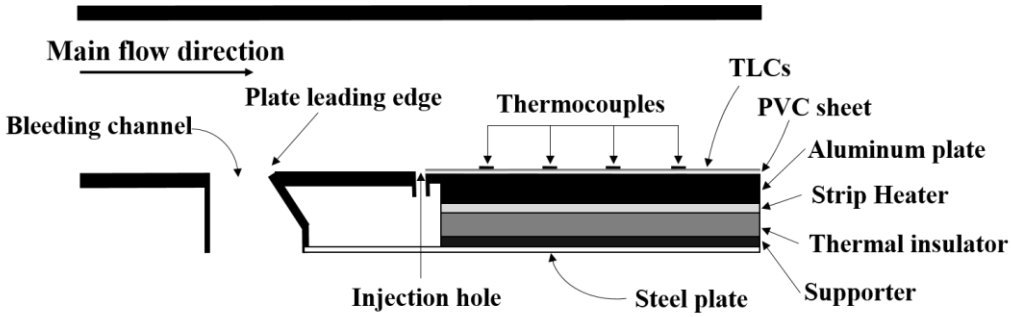

Fig. 2. Schematic diagram of test section in water tunnel.

The turbulent spot was created by a small jet, pulsed though a 1 mm diameter hole in perpendicular direction of the main stream flow. This hole locates at the streamwise distance of 0.3 m from the plate leading edge and directly connects with the pressure system as shown in Fig. 3. The water injection from the water tank is controlled with air pump, which is connected to the diaphragm tank to provide the constant pressure of the system. Then, the solenoid valve was used to control the injecting procedure by through programmable logic controller (PLC). The injecting interval was set at 0.01 s.

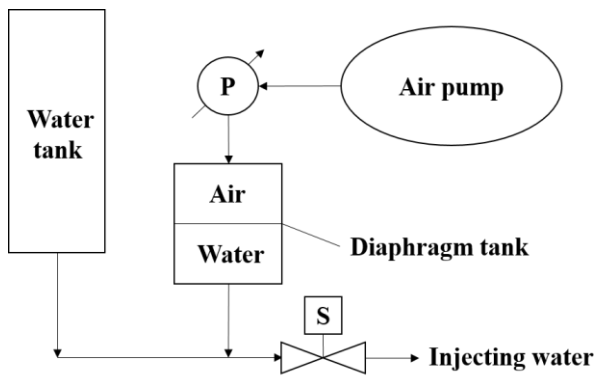

Fig. 3. Pressure system.

Finally, a fluorescent bulb having diameter of 2.5 cm was installed at each side of the test section. The white light, illuminating directly to the TLCs reflects a range of color from red to blue. These colors were recorded by video camera that is installed above test surface at 1.5 m. The frame rate of the image acquisition was set at 25 frames per second.

3.2 Mathematical analysis

In this study, the streamwise and spanwise distances are presented in dimensionless form by comparison to the diameter of injection hole as:

$$X = x / d \quad (1)$$

$$Y = y / d \quad (2)$$

Where X = dimensionless streamwise distance
x = streamwise distance from the plate leading edge (m)
Y = dimensionless spanwise distance
y = spanwise distance (m)
d = diameter of injection hole (m)

Moreover, the value of τ is the dimensionless time counted from the injection time. It is defined as the time in which the free stream water can move downstream with a streamwise distance of one diameter of the spot generator as:

$$\tau = t / (d / U_\alpha) \quad (3)$$

Where t = time, counted from the water injection (s)
U_α = freestream velocity (m/s)

In the test section, the images collected by video camera were found to be in RGB system, including Red, Green, and Blue signals. They can be changed into a system of HSI, which are Hue, Saturation, and Intensity signals, following Russ [5] as:

$$H = \cos^{-1}(Z) \quad \text{if} \quad G \geq R \quad (4)$$
$$H = 2\pi - \cos^{-1}(Z) \quad \text{if} \quad G < R \quad (5)$$
$$Z = (2B - G - R/2) / ((B - G)^2 + (B - R) / (G - R))^{1/2} \quad (6)$$

Where H = Hue signal value
R = Red signal value
G = Green signal value
B = Blue signal value

The Hue signal can be converted to a temperature value using a calibrated relation, fitted from the color-temperature calibration process. In order to perform this process, the water flow condition and the light setting must be kept as the test condition. Also, there was no water injection during the process. The color of the TLCs was recorded in RGB system in the window of 20 pixels x 20 pixels at the 2nd thermocouple tip. Each color was averaged and converted to Hue signal through the temperature of 26.3˚C – 29.6˚C with an interval of 0.3˚C. Before the record, the heat surface was left for about 15 minutes to reach the steady state heat transfer.

The relation between the obtained hue and temperature was fitted by 3rd order polynomial equation as shown in Fig 4. It is noted that the uncertainty of liquid crystals is also presented in the figure. The yielded equation can be presented as:

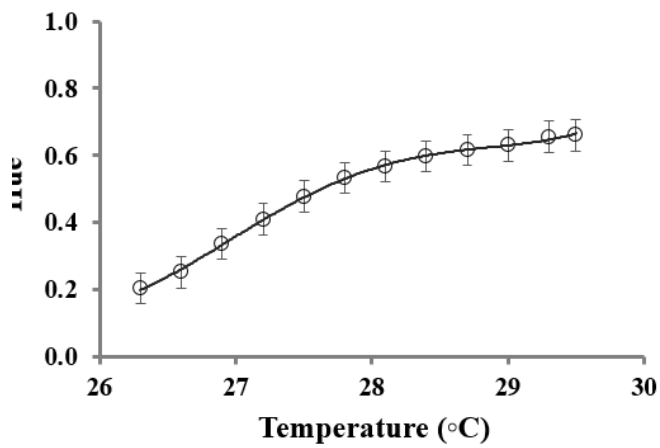

Fig. 4. The calibrated relation between hue and temperature.

$$T = 61.565H^3 - 67.807H^2 + 27.834H + 22.915 \quad (7)$$

Where T = the temperature on the heated surface (˚C)

Besides, this equation has a goodness of fit (R^2) of 0.99873. The local Reynolds number on the flat plate can be determined as:

$$Re_x = \rho U_\alpha x / \mu \quad (8)$$

Where ρ = density of water (kg/m^3)
μ = dynamic viscosity of water (kg/m.s)

The current experiment was carried out under the assumption, that the constant heat flux condition was applied to the test plate with the rate of 180 watts. Thus, the local heat transfer coefficient following Kays et al. [6] and Cengel and Ghajar [7] can be determined as:

$$h_x = (0.453Re_x^{1/2}Pr^{1/3})(k) / [1-(\xi/x)^{3/4}]^{1/3}(x) \quad (9)$$

$$q = Q / A \quad (10)$$

and

$$h_x = q / (T_s - T_\alpha) \quad (11)$$

Where h_x = local heat transfer coefficient ($W/m^2.^\circ C$)
Pr = Prandtl number
k = thermal conductivity ($W/m.^\circ C$)
ξ = unheated starting length (m)
Q = rate of heat transfer (W)
A = area of heated surface (m^2)
q = heat flux (W/m^2)
T_s = surface temperature ($^\circ C$)
T_α = freestream temperature ($^\circ C$)

The local heat transfer coefficient is validated by comparison with those determined from Eq. (9) at Re = 117,000, 158,000, and 199,000 as shown in Fig. 5. The figure shows that the h_x obtained by the present experiment agrees well with the results calculated from the correlation of Kays et al. [6].

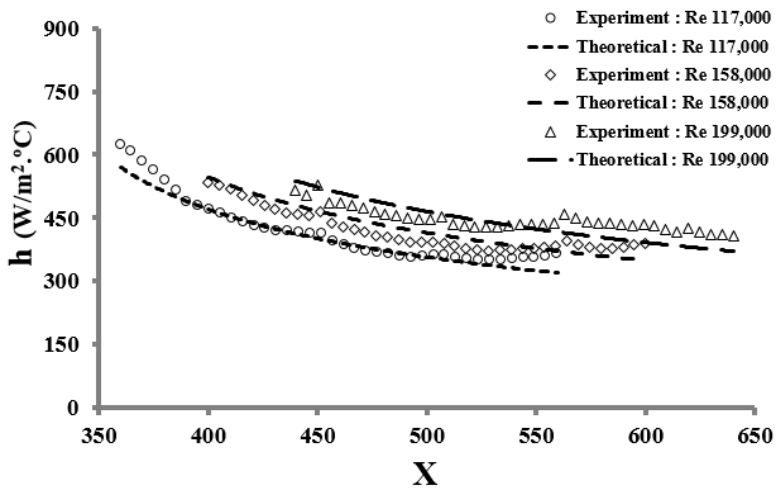

Fig. 5. Validation of the local heat transfer coefficient from the experiment and the results calculated by correlation of Kays et al. [6].

4. RESULTS AND DISCUSSIONS

In this study, the image processing technique was used to convert the signal of each pixel in the image. Firstly, the images of the test surface were recorded in RGB system as shown in Fig. 6 (d). The RGB signal contains Red, Green, and Blue signals as depicted in Fig. 6 (a), (b), and (c), respectively. However, HSI system including Hue, Saturation, and Intensity signals as shown in Fig. 6 (e), (f), and (g), respectively is found to be suitable for the image processing. In the current study, only Hue signal presenting the color was utilized to correlate with the temperature via Eq. (7) as depicted in Fig. 6 (h).

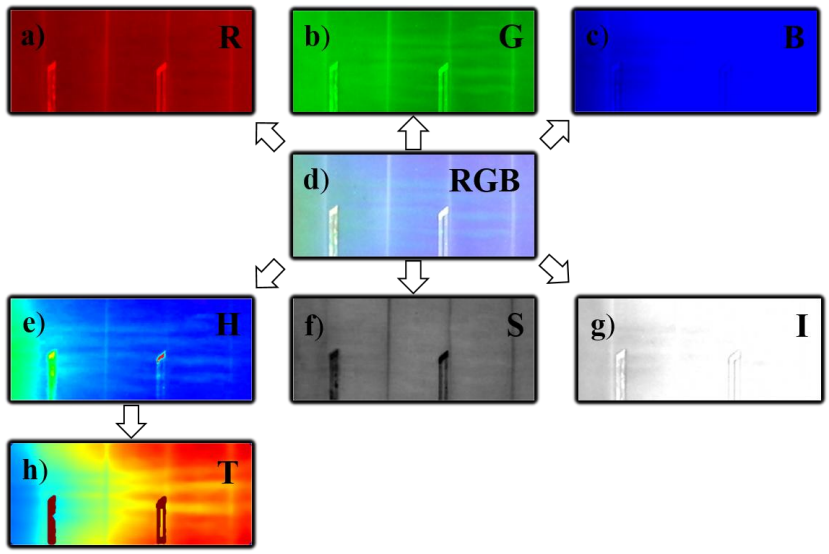

Fig. 6. Method of image processing.

Fig. 7 (a), (b), and (c) present the surface temperature contour at Re = 117,000, 158,000, and 199,000 of steady state condition. The water flows from left to right. It should be noted that the streamwise distance of each Re is specified differently depending on the Re. The blue patches appearing in each image present the location of the thin leaf thermocouple. Meanwhile, the dimensionless spanwise distance was set between -45 to 45. At each Re, the color bar presenting the temperature range is set equally between 26.2˚C – 30.2˚C. The figure shows that when the test plate was heated by a 180W plate heater, the temperature less increases along the streamwise direction at relatively higher Re. In each image, the maximum temperature was found as 30˚C, 29.5˚C, and 29˚C at Re = 117,000, 158,000, and 199,000, respectively.

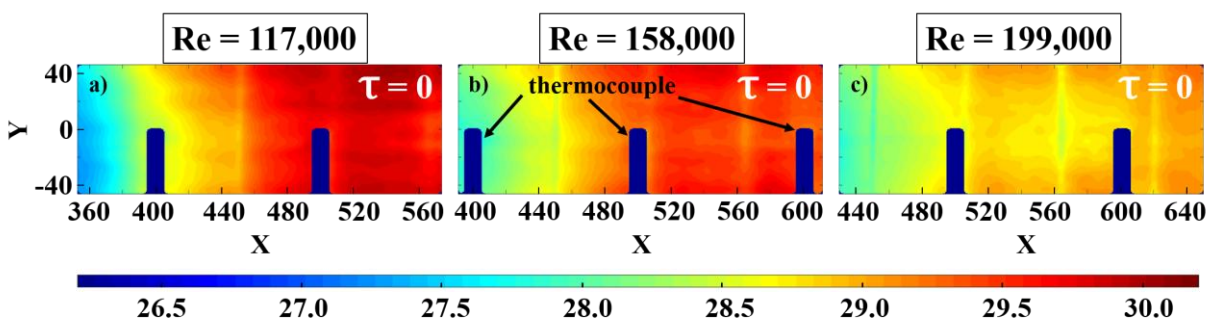

Fig. 7. Temperature contour on the test plate at Re = 117,000, 158,000, and 199,000.

Fig. 8 shows the contours of temperature after the water injection. From the figure, it is found that the turbulent spot is directly created from the injection and caused the decreasing of surface temperature. The evolution of the spot is presented since an arrival of the turbulent spot until it reaches a right edge of the image. Thus, the floating times are selected differently at each Re. The figure shows that the turbulent spot has the streaky structure under the constant heat flux condition. The temperature inside the turbulent spot decreases by the effect of hairpin vortices. Especially at the core of each streak, the relatively minimum temperature is found. However, some errors occur in the contours as a band in y-axis at the X = 460, 510, 570, and 620. It was caused from the discontinuity of the vanish cover. Even it is clearly found, the primary characteristics of the turbulent spot on the constantly heated plate can be seen.

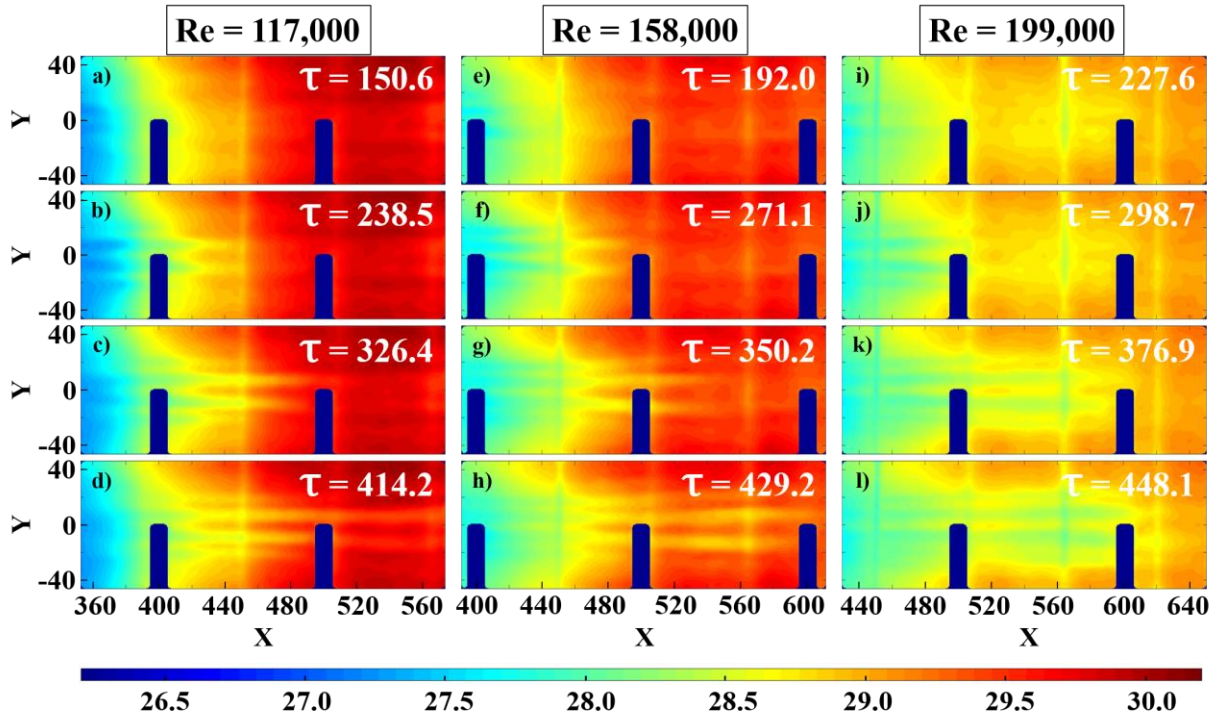

Fig. 8. Temperature contour at Re of 117,000, 158,000, and 199,000 with an arrival of turbulent spot.

The distributions of heat transfer coefficient on the test plate at Re = 117,000, 158,000, and 199,000 without the presence of the turbulent spot are presented as shown in Fig. 9 (a), (b), and (c), respectively. They were determined from the obtained surface temperature via Eq. (11). The value of the heat transfer coefficient on the surface is found between 350 – 650 W/m^2.˚C, which is in agreement with those obtain from the correlation, proposed by Kays et. al. [6].

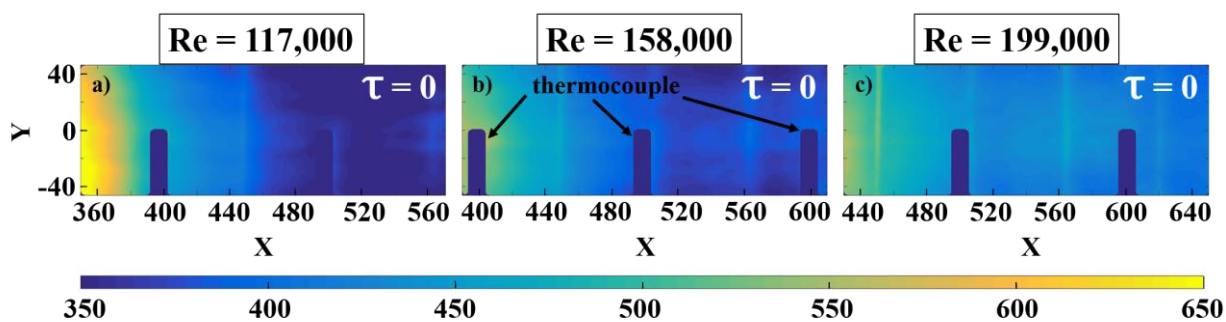

Fig. 9. Heat transfer coefficient contour on the test surface at Re = 117,000, 158,000, and 199,000.

Fig. 10 illustrates the contours of the heat transfer coefficient after an arrival of turbulent spot at Re = 117,000, 158,000, and 199,000. The results show that the convective heat transfer is enhanced via the vortices, generated after the water injection. Moreover, the contours show that the turbulent spot size under the higher Re is found to be relatively larger in spanwise direction. These present that the area of heat transfer via turbulent spot expands when the Re increases.

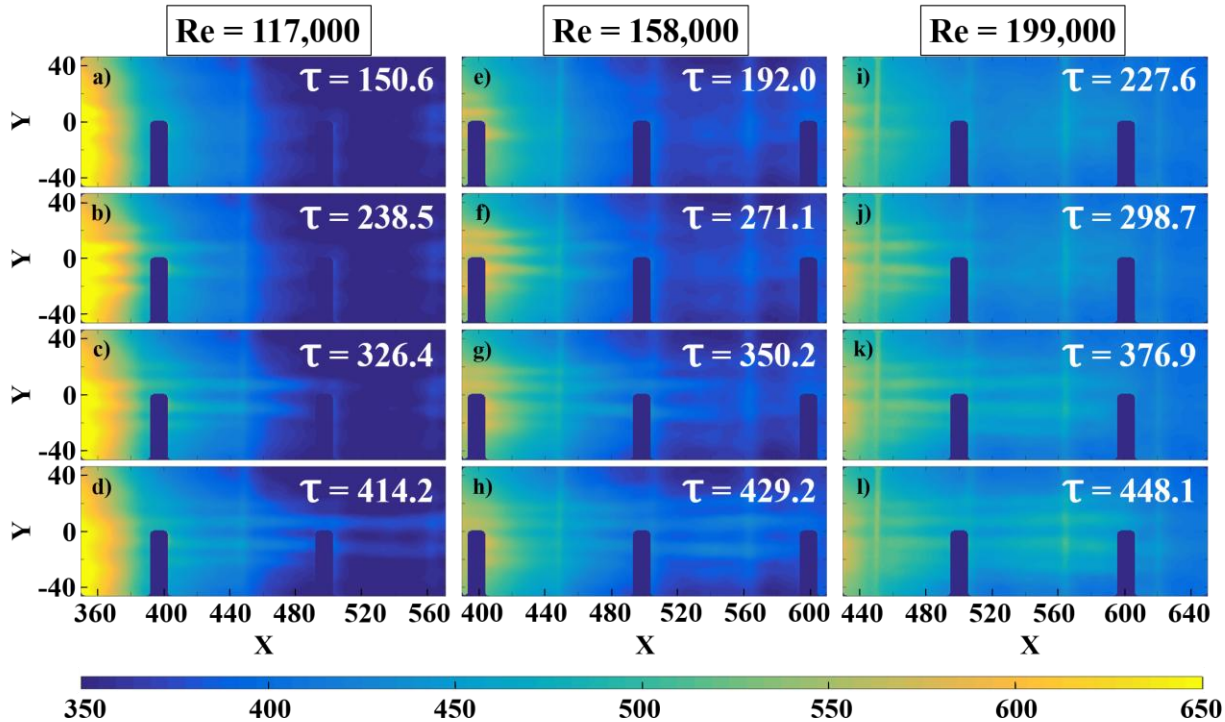

Fig. 10. Heat transfer coefficient contour at Re of 117,000, 158,000, and 199,000 with an arrival of turbulent spot.

The average and maximum values of heat transfer coefficient inside the turbulent spot can be extracted using image processing technique. Firstly, the bound of the spot can be evaluated by image subtraction of the temperature contour (Chaiworapuek et al. [8]) as depicted in Fig. 11. The figure shows that the turbulent spot structure is yielded as the temperature contour of the test surface with the spot subtracts with those without the spot.

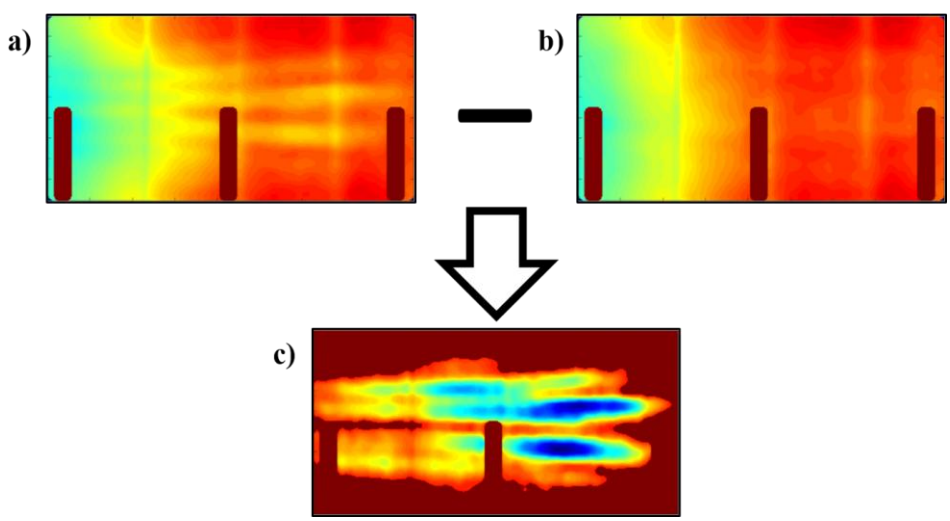

Fig. 11. Process of image subtraction.

Fig. 12 presents the average heat transfer coefficient inside the turbulent spot, h_{avg} against the τ, counted from the water injection. It is compared with the heat transfer coefficient of the laminar state, averaged in the bound of turbulent spot at the same moment. The h_{avg} is found to be higher above these in the laminar flow. Also, it is

decreasing with the increasing time. During the τ = 140 - 260, the h_{avg} is relatively higher for the lower Re. Conversely. It becomes relatively lower at the higher Re during the τ = 260 – 440.

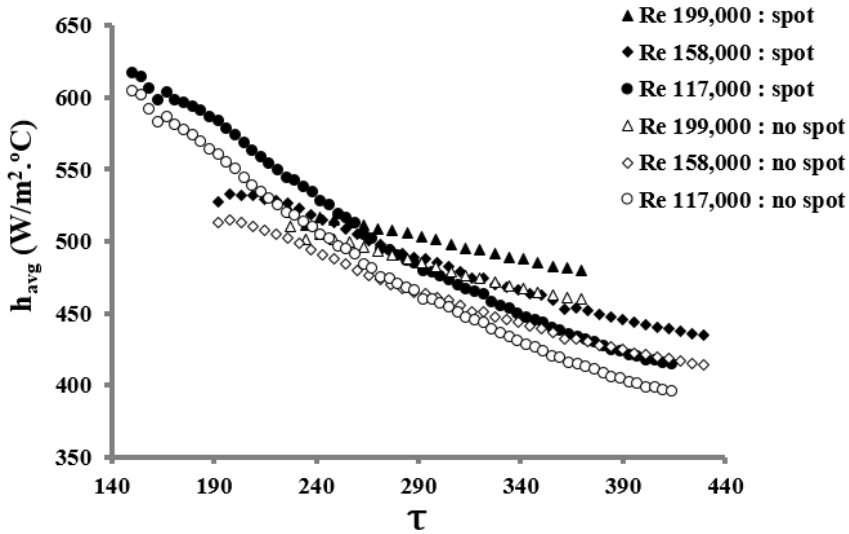

Fig. 12. The average heat transfer coefficient at Re of 117,000 158,000 and 199,000.

The maximum heat transfer coefficient inside the turbulent spot, h_{max} is also presented against the time as shown in Fig. 13. The difference between these with and without turbulent spot is about 20 - 50 W/m^2.$^\circ$C during the τ = 140 - 440. This difference decreases with the increasing time. The h_{max} at low Re is found to be higher than these at higher Re.

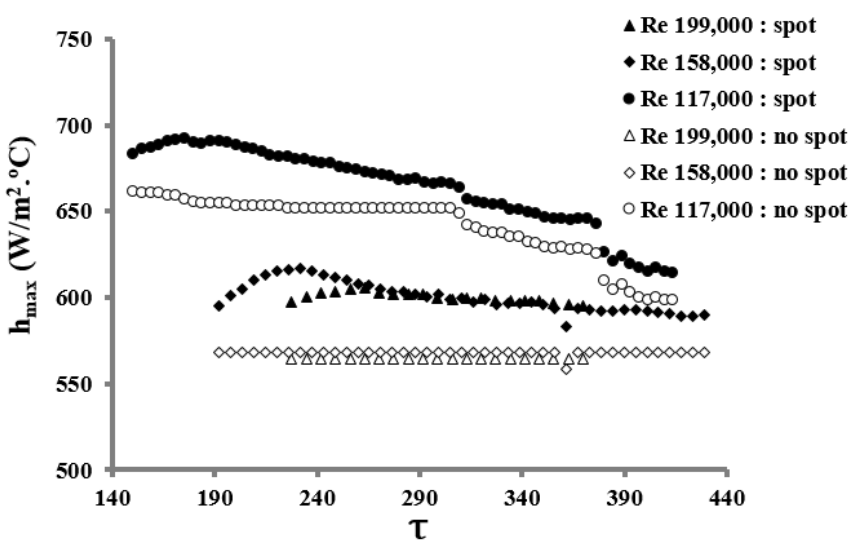

Fig. 13. The maximum heat transfer coefficient at Re of 117,000 158,000 and 199,000.

5. CONCLUSION

This study presents the technique of heat transfer enhancement using the small pulsating jet in perpendicular direction of the mainstream. The surface temperature at Re = 117,000, 158,000, and 199,000 under the constant heat flux condition was measured using the liquid crystals. The results show that the turbulent spot, generated from the water jet causes the increase of heat transfer rate. It has streaky structure and the relatively low temperature inside itself. Consequently, its heat transfer coefficient increases up to 8% comparing with those in laminar state.

However, it is also found that the average and maximum heat transfer coefficients inside the spot decrease when the Re increases. Conversely, the size of the turbulent spot increases with the increasing Re.

6. ACKNOWLEDGEMENT

The authors would like to acknowledge the financial support from the Thailand Research Fund (TRF) and gratefully thank Prof. Dr. Tanongkiat Kiatsirirote for the valuable advices.

REFERENCES

[1] White, F.M. Fluid Mechanics, 2nd edition, 1986, McGraw-Hill. New York.
[2] Emmons, H.W. The laminar-turbulent transition in a boundary layer Part 1. Journal of Aeronautical Science 18, 1951, pp. 490-498.
[3] Sabatino, D. and Smith, C.R. Simultaneous velocity-surface heat transfer behavior of turbulent spots, Experiments in Fluids, 2002, pp. 13-21.
[4] Chaiworapuek, W. and Kittichaikarn, C. On the thermal and structural characteristics of an artificially generated young turbulent spot, International Journal of Heat and Mass Transfer 92, 2016, pp. 850-858.
[5] Russ, J.C. The Image Processing Handbook, 4th edition, 2002, CRC. Boca Raton.
[6] Kays, W.M., Crawford, M.E., and Weigand, B. Convective Heat and Mass Transfer, 4th edition, 2005, McGraw-Hill. New York.
[7] Cengel, Y.A. and Ghajar, A.J. Heat and Mass transfer: Fundamentals & Applications, 5th edition, 2015, McGraw-Hill. New York.
[8] Chaiworapuek, W., Nongnoi S., and Kittichaikarn C. Heat transfer measurement on a turbulent spot using the energy balance method, Kasetsart Journal (Natural Science) 48 (4), 2014, pp. 1-14.